Available online at www.sciencedirect.com
ScienceDirect
Polymer 48 (2007) 5639–5645
polymer
www.elsevier.com/locate/polymer

Facile preparation of pH-responsive gelatin-based core–shell polymeric nanoparticles at high concentrations via template polymerization

Youwei Zhang*, Zhouxi Wang, Yansong Wang, Jiongxin Zhao, Chengxun Wu

State Key Laboratory for Modification of Chemical Fibers and Polymer Materials, Institute of Chemical Fibers, College of Material Science and Engineering, Donghua University, Shanghai 201620, China

Received 27 April 2007; received in revised form 13 July 2007; accepted 13 July 2007
Available online 26 July 2007

Abstract

Adopting gelatin as template macromolecules and acrylic acid (AA) as monomers, core–shell polymeric nanoparticles at a concentration of 30 mg/mL was successfully prepared via template polymerization, in which polymerization of the monomer and self-assembly between the polymer and the template take place simultaneously. The self-assembly was driven by specific interactions between gelatin and PAA produced in-situ, leading to nanoparticles with insoluble inter-polymer complexes of PAA and gelatin as the core and soluble gelatin as the shell. DLS and electrophoretic light scattering techniques were used to monitor the in-situ polymerization process, which indicated a size shrinkage and a surface charge decrease of the nanoparticles. The structure and morphology of the nanoparticles were characterized by FT-IR, TEM and SFM. The structure stability of the nanoparticles was improved by selectively crosslinking gelatin with glutaraldehyde. The nanoparticles also exhibit excellent pH–response: when pH changed from acid to base, the particles' volume expanded more than 80 times.

Keywords: Nanoparticles; Gelatin; Template polymerization

1. Introduction

Core–shell polymeric nanoparticles in nano and sub-micro scales have attracted much attention due to their potential applications in various fields. For example, they can be used as nano-carriers for catalysts, drugs, molecules with electronic and photonic functions, and biomolecules [1–3]. Emulsion polymerization is the most efficient way to prepare core–shell polymeric particles [4–7]. However, the removal of surplus surfactant, if possible, was very difficult; it is limited to vinylic monomers, and thus many bio-macromolecules and other water-soluble synthetic polymers cannot be used as the shell component.

Core–shell polymeric particles can also be fabricated via self-assembly routes, including the traditional micellization of amphiphilic block or graft copolymers in their selective solvents [8–12], environmental stimuli-induced micellization [13–17], chemical reaction-induced micellization [18,19], complexation-induced micellization [20–22], and routes to non-covalently connected micelles (NCCM) [23–25]. However, micellization is usually conducted at a low concentration (<5 mg/mL) and of low efficiency, which limits its practical application. Aimed at increasing the preparation efficiency, many new approaches have been explored. Armes fabricated stable shell-crosslinked micelles at a high concentration (100 mg/mL) from triblock copolymers [26,27]; Chen obtained core-crosslinked micelles at high concentrations by directly crosslinking one block of di-block copolymer in their co-solvent [19]. However, they all adopt block copolymer precursor, which is difficult to synthesize, and thus still hard to be used in practical production.

Recently, researchers' efforts are to develop more convenient way to prepare polymeric nanoparticles at high concentrations. Jiang synthesized hollow nanospheres via polymerizing acrylic acid in the presence of chitosan [28,29]; Li prepared smart microgels with pH-responsive shells and temperature-

* Corresponding author. Tel.: +86 21 67792889; fax: +86 21 67792855.
E-mail address: zhyw@dhu.edu.cn (Y. Zhang).

0032-3861/$ - see front matter © 2007 Elsevier Ltd. All rights reserved.
doi:10.1016/j.polymer.2007.07.046

responsive cores via aqueous graft copolymerization of *N*-isopropyl acrylamide (NIPAM) and *N*,*N*-methylenebisacrylamide(MBA) from water-soluble polymers at a temperature above the LCST of crosslinked PNIPAM [30].

In previous papers, we reported a convenient way to prepare thermo-sensitive polymeric core–shell nanoparticles at relatively high concentrations, i.e., polymerizing NIPAM and MBA on the surface of poly(ε-caprolactone) (PCL) nanoparticles at 76 °C [31,32]. The strategy of simultaneous polymerization and self-assembly was adopted in the procedure, that is, the polymerization of NIPAM and MBA and the self-assembly of crosslinked PNIPAM to the shell are simultaneous. Here, we reported our new progress in the strategy. Taking advantage of the simultaneous polymerization and self-assembly between the components driven by the specific interactions, a more facile procedure using macromolecules instead of PCL nanoparticles as the template, that is, template polymerization [33], was developed. Adopting gelatin as the template and acrylic acid (AA) as the monomer, through template polymerization, i.e., polymerization of AA in the gelatin aqueous solution, narrowly distributed biocompatible core–shell nanoparticles at a concentration of 30 mg/mL were prepared. The resultant nanoparticles have cores composed of insoluble PAA–gelatin inter-polymer complexes and shells of soluble gelatin, and their structures were further locked by selectively crosslinking gelatin with glutaraldehyde.

2. Experimental section

2.1. Materials

Acrylic acid (AA) of analytic grade was distilled under vacuum before use to remove the inhibitor. PAA was synthesized by AIBN-initiated free radical polymerization, with $M_n = 1.51 \times 10^5$ and $M_w/M_n = 2.99$ estimated by size exclusion chromatography in tetrahydrofuran. Gelatin (gelatin B) was a derived protein and obtained by partial hydrolysis of collagen via basic hydrolysis method, with $M_n = 1.52 \times 10^4$ and $M_w/M_n = 18.7$ estimated by GPC measurement in water. Initiator ammonium persulfate (APS), accelerator *N*,*N*,*N*′,*N*′-tetraethylmethylene diamine (TEMED, Acros), crosslinker glutaraldehyde (GA) (25% aqueous solution), NaOH and HCl were used as received. Cellulose membrane bag with a 14,000 cut-off molecular weight was purchased from Shanghai Green Bird Co. Ltd. Deionized water was used in all the experiments.

2.2. Preparation of PAA/gelatin nanoparticles

Gelatin was first dissolved in an aqueous HCl solution of pH 2.0, and then was filtered through a #3 sand-core funnel to remove insoluble impurities. Then, a certain amount of AA (the final concentration in the solution is 20 mg/mL) was added into 60 mL of the purified gelatin solution (10 mg/mL) under stirring in a nitrogen atmosphere. Polymerization was initiated at 40 °C by APS and TEMDE. The reaction was allowed to proceed for 180 min, followed by dialyzing against HCl solution with a pH same to that of the reaction solution (about 2.5) for 3 days to remove small molecule impurities, mainly unreacted acrylic acid.

2.3. Crosslinking of PAA/gelatin nanoparticles

A certain amount of glutaraldehyde (about 15 wt% of gelatin of the nanoparticles), as a crosslinking reagent for gelatin, was added dropwise to a stirred undialyzed PAA/gelatin nanoparticles' solution at 40 °C. The reaction mixture was kept stirring for 1.5 h, followed by dialyzing against HCl solution (pH 2.5) for 3 days to remove small molecule impurities including unreacted acrylic acid and glutaraldehyde.

2.4. Measurements

FTIR was used to analyze the structure and composition of PAA/gelatin nanoparticles. FTIR spectra of PAA, gelatin, uncrosslinked and crosslinked PAA/gelatin nanoparticles were obtained on a Nicolet Magna 550 spectrometer as KBr pellets. The average hydrodynamic diameter and zeta potential of PAA/gelatin nanoparticles were determined by dynamic light scattering (DLS) and electrophoretic light scattering using Malvern Zetasizer Nano ZS Particle Size and Zeta Potential Analyzer (DTS1060, Malvern, UK). The measurements were repeated three times and the results were the average of three runs. Morphology of the nanoparticles was observed by transmission electron microscopy (TEM) and scanning force microscopy (SFM). TEM observations were performed on a Philips CM 120 electron microscope at an accelerating voltage of 80 kV. The samples were prepared by placing 5 μl of stained nanoparticle solutions on copper grids, which were coated with thin films of Formvar and carbon, and allowing them to dry in the air. The nanoparticles were stained by sonification mixing of particles' solution and phosphate tungsic acid solution (5 wt%) for 10 min. SFM observations were conducted on a DI-NSIV scanning force microscope (Digital Instruments) using tapping mode. The sample preparation was similar to that for TEM except that freshly cleaved mica substrate was used.

The amount of PAA that is chemically grafted to gelatin in PAA/gelatin nanoparticles was determined as follows. First dissolve the nanoparticles by adjusting pH of the nanoparticles dispersion to around 8, followed by adding acetone to precipitate the product from the solution. After washing with lots of acetone and drying under vacuum, the product was extracted with ethanol to remove free PAA. The element N contents in the extracted product and gelatin (both dried at 100 °C before measurement) were measured by a Elementar Vario EL III element analysis, from which the amount of PAA chemically grafted to gelatin was calculated.

3. Results and discussion

3.1. Micellization induced by complexation between PAA and gelatin

The inter-polymer complexation, due to specific interactions such as hydrogen bonding and electrostatic interaction

between the components, usually leads to the formation of macro-precipitates [34–36]. However, when natural macromolecule derivate, which bears two or more kinds of functional groups, was adopted as one of the components, stable core–shell micelles or nanoparticles could be obtained [22,37,38]. For example, via changing medium pH, Jiang obtained stable core–shell micelles, with insoluble inter-polymer complexes of HEC and PAA grafts as the core and free HEC as the shell, from a graft copolymer of hydroxyethyl cellulose and PAA (HEC-*g*-PAA) [22].

Gelatin is a derived protein with good biocompatibility and biodegradability, obtained by partial hydrolysis of collagen. Gelatin B used here was produced by a basic hydrolysis method with an isoelectric point (IP) about 4.8. That is, gelatin macromolecules are positively charged when pH > 4.8, while negatively charged when pH < 4.8. When adding 0.5 mL of 1 mg/mL PAA solution dropwise into 5 mL of 1 mg/mL gelatin solution at pH 2 under stirring, a bluish tint appeared, indicating the formation of nanoparticles. DLS result revealed that the nanoparticles with an average hydrodynamic diameter about 216 nm formed from the micellization induced by the complexation between PAA and gelatin. Upon adding PAA solution, due to hydrogen bonding interactions between unionized carboxyl groups of PAA and carbonyl groups of gelatin and electrostatic interactions between ionized carboxyl groups of PAA and protonated amino groups of gelatin, PAA complexed with gelatin and formed insoluble inter-polymer complexes. The hydrophobic complexes would aggregate to form precipitates. However, no macro-precipitates were observed, suggesting the aggregates were stabilized by soluble macromolecules. We believed that, since gelatin bears several hydrophilic groups such as amino, carboxy, and hydroxyl, some gelatin macromolecules remained soluble after interacting with PAA locally and hence stabilized the aggregates. As a result, micelles with inter-polymer complexes of PAA and gelatin as the core and gelatin as the shell formed.

Micellization is usually conducted at a low concentration; otherwise, large irregular aggregates or even precipitates will produce. This is because micellization at a relatively high concentration occurs so rapidly that there is no enough time for the soluble chains to disentangle and adjust their confirmation so as to surround the insoluble aggregates, thus leading to larger and even irregular aggregates. So is the case for the micellization induced by the complexation between PAA and gelatin. When the concentrations of both PAA solution and gelatin solution increased to 5 mg/mL and 10 mg/mL, the size of the resultant particles increased to about 522 nm and 1006 nm, respectively. Therefore, slowing down the formation of insoluble inter-polymer complexes between PAA and gelatin and their subsequent aggregation is the key factor to produce PAA/gelatin nanoparticles with well-defined structure at high concentrations via micellization.

Here, we took advantage of the simultaneous polymerization and self-assembly in the template polymerization, which can slow down the self-assembly between the components, to prepare core–shell polymeric nanoparticles at high concentrations. As illustrated in Scheme 1, core–shell PAA/gelatin nanoparticles were prepared via in-situ polymerization of AA in the presence of template gelatin macromolecules, followed by selective crosslinking of gelatin to lock the nanoparticles' structure.

3.2. Preparation of PAA/gelatin nanoparticles via template polymerization

3.2.1. Formation of PAA/gelatin nanoparticles during template polymerization

Using gelatin as template macromolecules and AA as monomers, narrowly distributed nanoparticles at a fairly high concentration (30 mg/mL) were prepared successfully via template polymerization. To analyze the forming mechanism of nanoparticles during the template polymerization, dynamic light scattering and electrophoretic light scattering techniques were used to follow the polymerization process. The starting gelatin/AA solution was transparent, and a bluish tint, which indicates the formation of nanoparticles, appeared and became deeper as the reaction proceeded. Fig. 1 illustrated the hydrodynamic diameter distribution curves of the reaction solution at different stages. When the reaction took place for 20 min, there were two peaks in the distribution curve. The main peak corresponds to the PAA/gelatin nanoparticles formed via self-assembly between PAA produced in-situ and gelatin, and the minor peak possibly the soluble complexes of AA and gelatin. As the polymerization proceeded, on the one hand, the area of the minor peak decreased and only the main particles were detected by DLS after the polymerization proceeded for 70 min; on the other hand, the particles

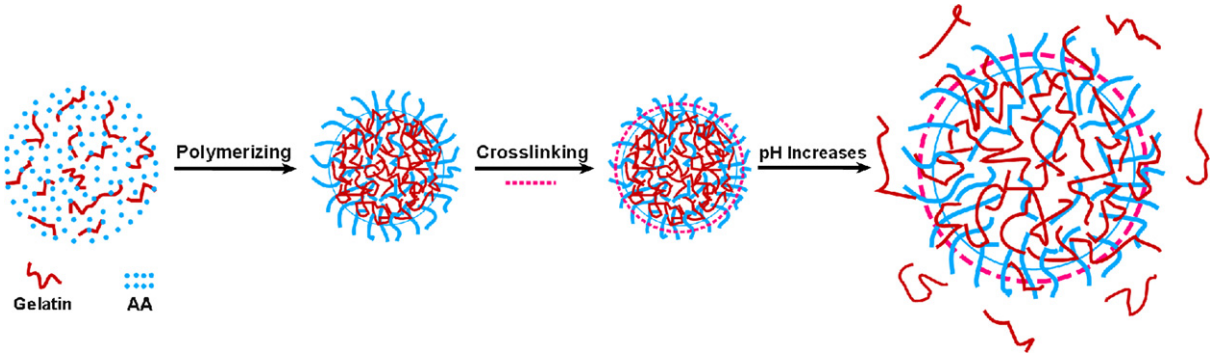

Scheme 1. Schematic illustration for preparing core–shell PAA/gelatin nanoparticles at high concentrations.

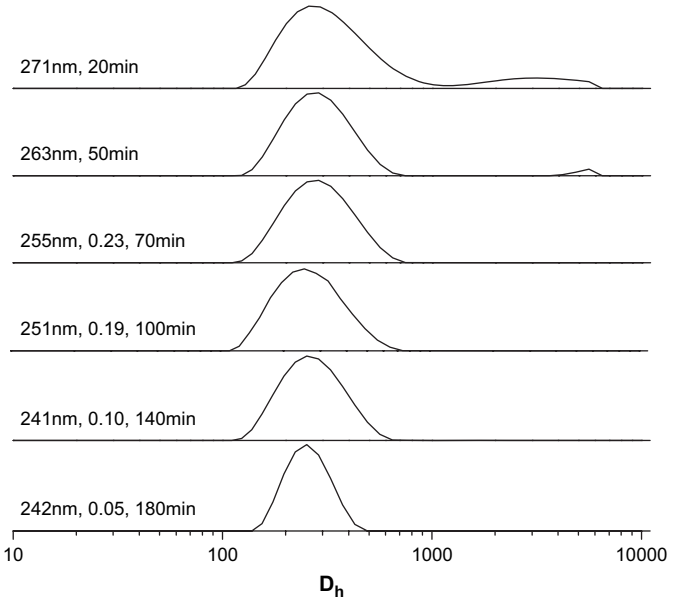

Fig. 1. Hydrodynamic diameter distribution curves of the reaction solution at different polymerization stage. Three numerals listed in the left denote the average hydrodynamic diameter ($\langle D_h \rangle$), polydispersity index (PDI) and polymerization time, respectively.

contracted slowly, accompanied by a decrease in the polydispersity index (PDI) of the particle size. The $\langle D_h \rangle$ and PDI at the end of the polymerization were around 240 nm and 0.05, respectively.

The change in the ζ-potential of the reaction solution during the polymerization was similar to that of $\langle D_h \rangle$ (Fig. 2), i.e., the ζ-potential fell down rapidly from an initial value of 14.7 mV to around 11.8 mV in the first 20 min, and then decreased slowly to around 11.0 mV at the end of the polymerization. The decreasing of the ζ-potential with the polymerization time revealed the electrostatic interactions between PAA produced in-situ and gelatin. Furthermore, the ζ-potential of the solution through the whole polymerization remained

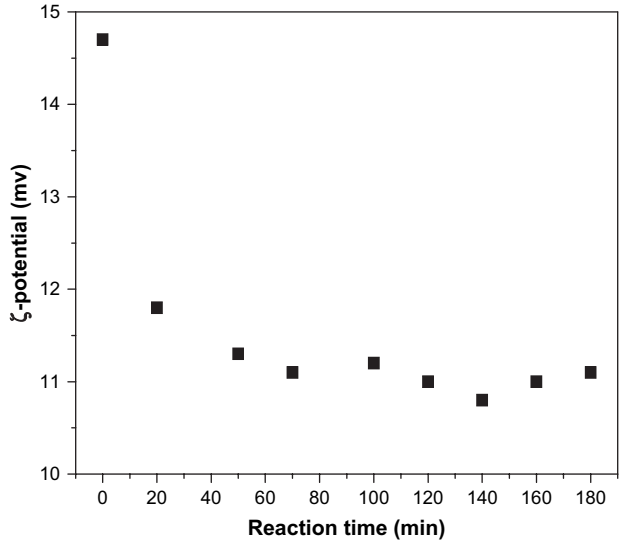

Fig. 2. ζ-Potential of the solution as a function of the reaction time.

positive, suggesting that gelatin macromolecules with protonated amino groups lying on the surface of the particles. The positive charges carried by soluble gelatin shell chains make PAA/gelatin core–shell nanoparticles exist stable in the water, and their secondary aggregations are prevented.

Upon adding AA to the gelatin solution, soluble complexes with loose structure would form due to the specific interactions between the components. When raising temperature to initiate the reaction, some AA monomers were first converted to PAA, which self-assembled with template gelatin to core–shell PAA/gelatin nanoparticles via the specific intermolecular interactions. As the polymerization continued, more and more PAA/gelatin nanoparticles formed. Therefore, the size of the particles of the solution decreased slightly further and the size distribution became narrower. In the template polymerization, as the conversion of AA monomers to PAA and the subsequent formation of PAA/gelatin nanoparticles took place little by little, the self-assembly between PAA and gelatin was slowed down. Therefore, core–shell PAA/gelatin nanoparticles can be prepared at fairly high concentrations via template polymerization. According to our further experimental results, which will be reported elsewhere, the preparation concentration could reach as high as 100 mg/mL via optimization of the reaction parameters.

The core–shell PAA/gelatin nanoparticles are co-stabled by hydrogen bonding and electrostatic interactions. As mentioned above, the electrostatic interactions between PAA and gelatin of the nanoparticles were proved by the ζ-potential results of the nanoparticles (Fig. 2). While the hydrogen bonding interactions in the nanoparticles were confirmed by infrared spectra results, the peak assigned to carbonyl stretching of carboxyl shifts from 1710 cm^{-1} for pure PAA to 1723 cm^{-1} for nanoparticles; meanwhile, the amide I band assigned to carbonyl stretching and the amide II band assigned to N–H bending shift from 1647 cm^{-1} and 1541 cm^{-1} for pure gelatin to 1643 cm^{-1} and 1536 cm^{-1} for nanoparticles, respectively (Fig. 3). In addition, when pH of the nanoparticle solution was adjusted to around 1.0 to destroy electrostatic interactions between gelatin and PAA [39], the bluish tint of the solution remained, indicating that hydrogen bonding interactions alone were strong enough to stabilize the particles in strong acid media.

In addition, the element analysis results showed that the N contents of gelatin and the extracted product (see Section 2.4) were 16.53% and 8.799%, respectively, from which it was determined that about 88% of PAA (based on the weight of gelatin) was chemically grafted to gelatin in the nanoparticles. This indicates that beside the specific interactions, there are also many chemical covalent connections between PAA and gelatin of the nanoparticles.

3.2.2. pH-responsive behavior of PAA/gelatin nanoparticles

The obtained core–shell PAA/gelatin nanoparticles are quite stable: there was almost no change in the size after storing for 15 days and only a minor decrease in the size (about 20 nm) was observed when diluted by 49 volumes of HCl solution with a same pH (pH 2.5) (data not shown).

As revealed above, the core–shell PAA/gelatin nanoparticles are co-stabilized by the electrostatic interactions and

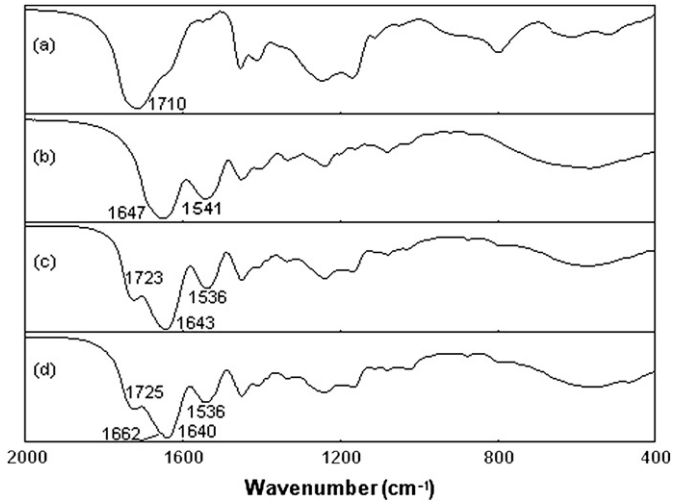

Fig. 3. Infrared spectra of PAA (a); gelatin (b); core–shell PAA/gelatin nanoparticles (c) and crosslinked PAA/gelatin nanoparticles (d).

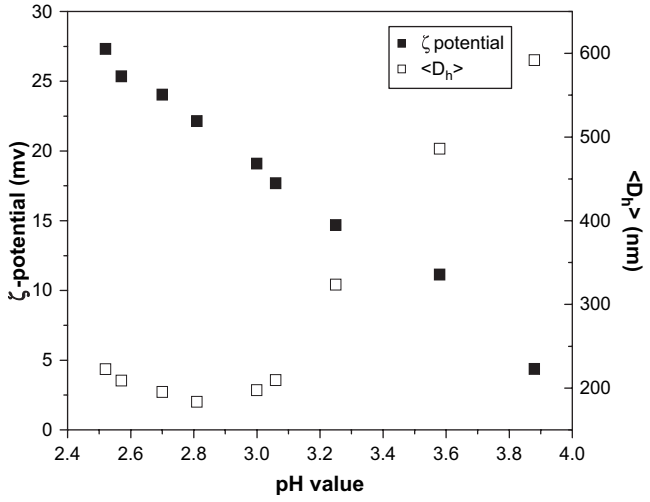

Fig. 4. $\langle D_h \rangle$ and ζ-potential of PAA/gelatin nanoparticles' solution with different pH, pH of the solution was adjusted by adding NaOH solution to the starting solution with a pH about 2.5 and a concentration 0.6 mg/mL.

hydrogen bonding interactions, which closely depend on pH of the medium. Therefore, it is interesting to study pH-responsive behavior of the nanoparticles. As displayed in Fig. 4, accompanying the continuous decrease in the ζ-potential, the particles' size first decreased slightly with increasing pH value until reaching a minimum at pH about 2.8, and then increased rapidly. As pH increased, the ζ-potential of the particles decreased, and the repulsion between the protonated amino groups of the particles' shell decreased, causing a slight contraction in the particles' shell, thus leading to the initial size decrease. However, when pH value increased above 3.0, the surface charge of the particles decreased to be too low to stabilize the particles, and there began to appear obvious aggregations between the particles. Therefore, the particle size increased rapidly. Macro-precipitation took place when pH value increased near the isoelectric point (IP) of the particles. Upon further increase in pH, PAA/gelatin particles would disintegrate due to the decomplexation between PAA and gelatin.

3.2.3. Morphology of PAA/gelatin nanoparticles

TEM is a powerful tool for observing morphologies of polymeric assembled objects. Without staining, we could barely see spherical particles in TEM micrograph of PAA/gelatin nanoparticles due to the low contrast between the particles and the background (Figure not shown). It was reported that phosphate tungsic acid (PTA)-staining technique can make core–shell structure visible for composite latexes by TEM [40]. Hence PTA was adopted to stain PAA/gelatin nanoparticles and a typical TEM micrograph of stained nanoparticles was given in Fig. 5a. It can be seen that, after staining, nanoparticles with slightly deformed round contours were observed. Furthermore, due to the selective staining of gelatin with PTA, the core–shell structure of the particles was disclosed, although the contrast between the core and shell was fairly weak. This again proved that the nanoparticles shells are mainly composed of gelatin chains.

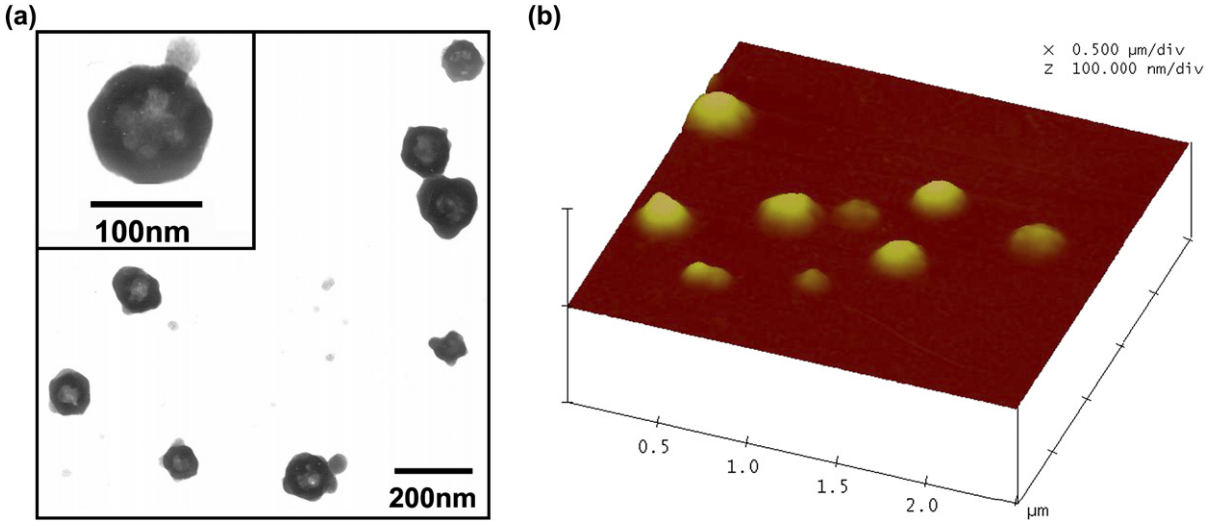

Fig. 5. (a) TEM micrograph of core–shell PAA/gelatin nanoparticles stained with phosphate tungsic acid, the inset is for a typical nanoparticle at a large magnification; (b) SFM micrograph of core–shell PAA/gelatin nanoparticles.

The nanoparticle size in TEM micrograph ranged from about 71 to 102 nm and was much smaller than its corresponding size measured by DLS (100–500 nm, $\langle D_h \rangle = 220$ nm). This is common for core–shell nanoparticles and is caused by the shrinking of the nanoparticles during the sample preparation [22,41,42]. Fig. 5b shows the typical SFM morphology of the nanoparticles. The nanoparticles' diameters ranged from about 122 to 340 nm, while their heights ranged from about 27 to 52 nm, indicating that the particles collapsed and spread on the mica surface.

3.3. Crosslinking PAA/gelatin nanoparticles with glutaraldehyde

To improve their structure stability, we further locked the structure of PAA/gelatin nanoparticles by selective crosslinking. GA was chosen to selectively crosslink gelatin through a reaction between the amino groups of gelatin molecules and aldehyde groups of GA molecules [43,44]. After selective crosslinking, there was a slight shrinkage in the particles' size from the original 242 nm to 227 nm. In addition, a new small peak around 1662 cm^{-1} assigned to N=C stretching appeared in FTIR spectrum of the crosslinked nanoparticles (see Fig. 3). The dilution experimental results indicated that the decrease in size of the particles after crosslinking with dilution became lesser: there was only a size decrease about 7 nm when diluted to 1/50 concentration (data not shown).

3.3.1. pH-responsive behavior of crosslinked PAA/gelatin nanoparticles

The pH dependence of the size of the crosslinked PAA/gelatin nanoparticles was also studied, and the result is shown in Fig. 6. The main features of Fig. 6 are as follows. First, after selectively crosslinking gelatin with GA, the PAA/gelatin particles remained in the near neutral and basic medium, indicating that the structure of the particles was successfully locked by crosslinking. Second, the size change of the crosslinked particles with pH below its IP was similar to that of uncrosslinked ones. Third, above its IP, due to the decomplexation between PAA and gelatin, the crosslinked particles expanded greatly. And due to the repulsion interactions between the ionized carboxyl of gelatin and PAA, the particles' size continued to increase rapidly as pH increased. Obviously, the crosslinked particles exhibited good pH–response: when pH of the solution changed from 2.5 to around 8, the particles' size increased from 220 nm to about 960 nm, i.e., the particles' volume expanded more than 80 times.

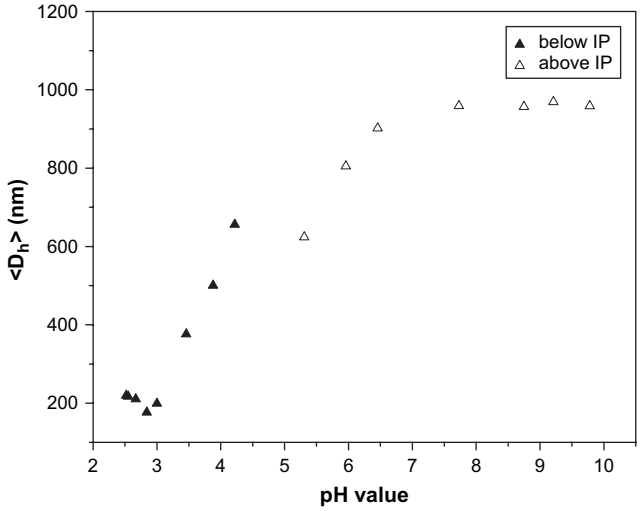

Fig. 6. $\langle D_h \rangle$ of crosslinked PAA/gelatin nanoparticles' solution at different pH, pH of the solution was adjusted by adding NaOH solution to the starting solution with a pH value of about 2.5 and a concentration of 0.6 mg/mL. Solid and hollow points are denoted for data points below and above the IP of the nanoparticles, respectively.

3.3.2. Morphology of crosslinked PAA/gelatin nanoparticles

The morphology of the crosslinked PAA/gelatin nanoparticles was also observed with TEM and SFM (Fig. 7). Comparing TEM micrograph of the crosslinked nanoparticles (Fig. 7a) with that of uncrosslinked ones (Fig. 5a), it can be seen that,

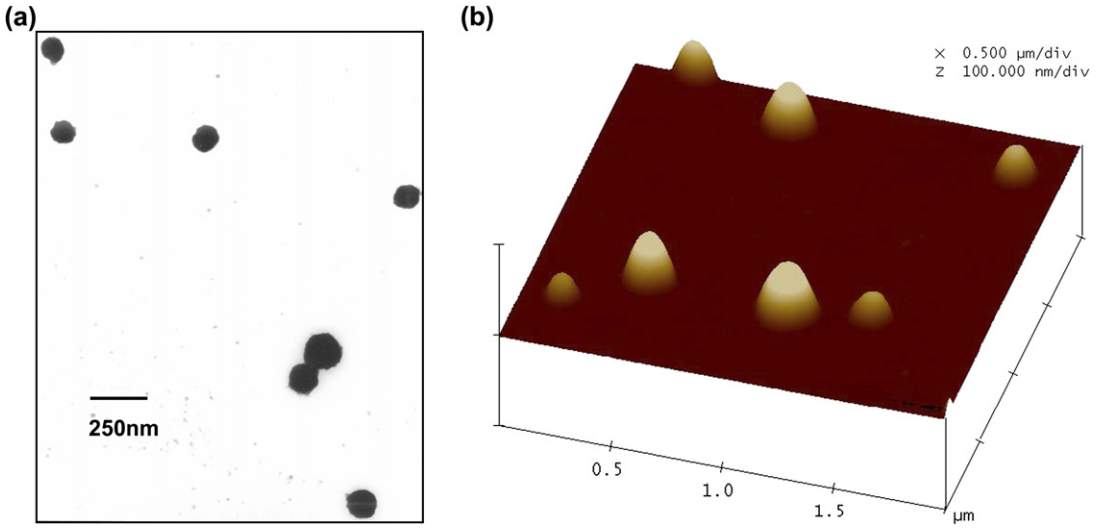

Fig. 7. (a) TEM micrograph of crosslinked core–shell PAA/gelatin nanoparticles stained with phosphate tungsic acid; (b) SFM micrograph of crosslinked core–shell PAA/gelatin nanoparticles.

after crosslinking, the core–shell structure of the nanoparticles was no longer discerned and the nanoparticles' contours became more circular. Fig. 7b displays the SFM morphology of the crosslinked nanoparticles. The particles in SFM micrograph had diameters ranging from about 155 to 292 nm and heights from about 56 to 107 nm. By comparing with Fig. 5b, we can see that the crosslinked nanoparticles collapsed less on the mica substrate, indicating that the stiffness of gelatin shell can be improved by crosslinking.

4. Conclusions

Adopting AA as the monomers and gelatin as the template, narrowly distributed PAA/gelatin nanoparticles with insoluble PAA–gelatin inter-polymer complexes cores and soluble gelatin shells were prepared at a high concentration via template polymerization, in which the polymerization of AA and the self-assembly between PAA and gelatin occurred simultaneously and thus slowing down the self-assembly of the components. The core–shell structure of the nanoparticles was confirmed by TEM observation. Furthermore, glutaraldehyde was adopted as a selective crosslinker to lock the nanoparticles' structure. The resultant crosslinked PAA/gelatin nanoparticles were pH-responsive: when pH of the solution changed from 2.5 to about 8.0, the volume of the particles expanded more than 80 times. The pH-sensitivity and biocompatible gelatin shell will surely make the resultant particles an attractive candidate for applications in biomedical field. In addition, many macromolecules and monomers easily available can be adopted to prepare core–shell nanoparticles with desirable properties in a complete aqueous solution via template polymerization.

Acknowledgements

This work was supported by the National Natural Science Foundation of China (NNSFC No. 20604006) and Director Foundation of State Key Laboratory for Modification of Chemical Fibers and Polymer Materials. The authors also thank Prof. Ming Jiang of Fudan University for his helpful discussion; and Prof. Meifang Zhu of Donghua University for her kind help in the experiments.

References

[1] Savic R, Luo LB, Eisenberg A, Maysinger D. Science 2003;300:615–8.
[2] Discher DE, Eisenberg A. Science 2002;297:967–73.
[3] Legrand P, Barratt G, Mosqueira V, Fessi H, Devissaguet JP. STP Pharm Sci 1999;9:411–8.
[4] Castelvetro V, De Vita C. Adv Colloid Interface Sci 2004;108:167–85.
[5] Xiao XC, Chu LY, Chen WM, Wang S, Li Y. Adv Funct Mater 2003; 13:847–52.
[6] Jang J, Ha H. Langmuir 2002;18:5613–8.
[7] Pavlyuchenko NV, Sorochinskaya OV, Ivanchev SS, Klubin VV. J Polym Sci Polym Chem 2001;39:1435–55.
[8] Gao A, Liu GJ, Tao J. Macromolecules 1996;29:2487–93.
[9] Zhao JX, Allen C, Eisenberg A. Macromolecules 1997;30:7143–50.
[10] Webber SE. J Phys Chem B 1998;102:2618–26.
[11] Huang HY, Remsen EE, Kowalewski T, Wooley KL. J Am Chem Soc 1999;3805–6.
[12] Stewart S, Liu GJ. Chem Mater 1999;11:1048–54.
[13] Ding H, Wu F, Huang Y, Zhang ZR, Nie Y. Polymer 2006;47:1575–83.
[14] Zhang JX, Qiu LY, Zhu KJ, Jin Y. Macromol Rapid Commun 2004; 25:1563–7.
[15] Weaver JVM, Armes SP, Bütün V. Chem Commun 2002;18:2122–3.
[16] Gohy JF, Antoun S, Jérôme R. Macromolecules 2001;34:7435–40.
[17] Martin TJ, Prochazka K, Munk P, Webber SE. Macromolecules 1996; 29:6071–3.
[18] Wu C, Niu AZ, Leung LM, Lam TS. J Am Chem Soc 1999;121:1954–5.
[19] Chen DY, Peng HS, Jiang M. Macromolecules 2003;36:2576–8.
[20] Harada A, Kataoka K. Macromolecules 1998;31:288–94.
[21] Liu SY, Armes SP. Angew Chem Int Ed 2002;41:1413–6.
[22] Dou HJ, Jiang M, Peng HS, Chen DY, Hong Y. Angew Chem Int Ed 2003;42:1516–9.
[23] Wang M, Zhang GZ, Jiang M, Chen DY. Macromolecules 2001;34:7172–8.
[24] Liu SY, Jiang M, Liang HJ, Wu C. Polymer 2000;41:8697–702.
[25] Zhao HY, Gong J, Jiang M, An YL. Polymer 1999;40:4521–5.
[26] Bütün V, Billingham NC, Armes SP. J Am Chem Soc 1998;120: 11818–9.
[27] Liu SY, Armes SP. J Am Chem Soc 2001;123:9910–1.
[28] Hu Y, Jiang XQ, Ding Y, Chen Q, Yang CZ. Adv Mater 2004;16:933–7.
[29] Hu Y, Chen Y, Chen Q, Zhang LY, Jiang XQ, Yang CZ. Polymer 2005;46:12703–10.
[30] Leung MF, Zhu JM, Harris FW, Li P. Macromol Rapid Commun 2004; 25:1819–23.
[31] Zhang YW, Jiang M, Zhao JX, Ren XW. Adv Funct Mater 2005;15:695–9.
[32] Zhang YW, Zhao JX, Jiang M, Wang JY. Chem J Chin Univ 2006;27: 1762–6.
[33] Połowiński SP. Prog Polym Sci 2002;27:537–77.
[34] Mun GA, Nurkeeva ZS, Khutoryanskiy VV. Macromol Chem Phys 1999;200:2136–8.
[35] Mun GA, Nurkeeva ZS, Khutoryanskiy VV, Sarybayeva GS, Dubolazov AV. Eur Polym J 2003;39:1687–91.
[36] Chun MK, Cho CS, Choi HK. J Appl Polym Sci 2004;94:2390–4.
[37] Chen Q, Hu Y, Chen Y, Jiang XQ, Yang YH. Macromol Biosci 2005;5:993–1000.
[38] Hu Y, Jiang XQ, Ding Y, Ge HX, Yuan YY, Yang CZ. Biomaterials 2002; 23:3193–201.
[39] Jiang HL, Zhu KJ. J Appl Polym Sci 2001;80:1416–25.
[40] Li XQ, Chen PZ, Qin CH, Liao SX. Polym Mater Sci Eng 1999;15:129–31 [in Chinese].
[41] Zhang YW, Jiang M, Zhao JX, Zhou J, Chen DY. Macromolecules 2004; 37:1537–43.
[42] Zhang YW, Jiang M, Zhao JX, Wang ZX, Dou HJ, Chen DY. Langmuir 2005;21:1531–8.
[43] Knaul JZ, Hudson SM, Creber KM. J Polym Sci Part B 1999;37:1079–94.
[44] Leo E, Vandelli MA, Cameroni R, Forni F. Int J Pharm 1997;155:75–82.